CrystEngComm

Accepted Manuscript

This article can be cited before page numbers have been issued, to do this please use: S. Alapour, S. Zamisa, J. R. A. Silva, C. N. Alves, B. Omondi, D. Ramjugernath and N. A. A. Koorbanally, *CrystEngComm*, 2018, DOI: 10.1039/C8CE00094H.

ROYAL SOCIETY OF CHEMISTRY

rsc.li/crystengcomm

View Article Online
DOI: 10.1039/C8CE00094H

Journal Name

ARTICLE

Investigations into the flexibility of the 3D structure and rigid backbone of quinoline by fluorine addition to enhance its blue emission

Received 00th January 20xx,
Accepted 00th January 20xx

DOI: 10.1039/x0xx00000x

www.rsc.org/

S. Alapour,[a] S. J. Zamisa,[a] J. R. A. Silva,[b] C. N. Alves,[b] B. Omondi,[a] D. Ramjugernath[c] and N. A. Koorbanally*[a]

Achieving the desired structures of organic molecules for targeted applications is vital. Folding caused by weak intermolecular forces plays an important part in their 3D structure. The discovery of powerful tools which enable us to do this are currently under investigation by researchers across the globe. In this account, quinoline was chosen as a model scaffold for having a rigid 3D structure. Addition of fluorine was found to result in increased flexibility of the structure with a decrease in the number of intermolecular interactions. This resulted in improvement of their photophysics and blue emission. A total of 19 novel fluoroquinoline molecules were synthesised in order to carry out this study. Of these, growth crystals of 10 compounds were successfully achieved and used. In addition, characterisation techniques such as NMR, HRMS, UV-Vis and computational techniques were used to explore the 3D structure of these molecules.

Introduction

Quinoline is a nitrogen containing heterocyclic aromatic compound, which has attracted the attention of medicinal and synthetic chemists for decades due to its various pharmaceutical applications. Quinoline and its derivatives have also been reported to have highly fluorescent and electroluminescent applications in the blue emission range (400-500 nm).[1] Industrial applications of quinolines such as dyes, preservatives and ligand to metal complexes have made an impact in luminescence chemistry.[2] Despite numerous publications on quinoline derivatives, there is still a large gap in the explanation of how substitution of different electron withdrawing and donating groups at different positions effect the conformation of quinoline and intermolecular interactions. The different conformations brought about by various substituents may have an influence on bioactivity and photophysical properties.

Fluorine in organic molecules has unique features, including good thermal and oxidative stability,[3] inverted charge density distribution,[4] and increased biological activity.[5] Consequently, fluorinated organic compounds also have potential application in organic light-emitting diodes (OLEDs)[6], organic photovoltaic devices (OPV)[7] and organic field-effect transistors (OTFT).[8] Synthesis of highly efficient blue-light emission organic material still remains a challenge as it has a higher band gap in comparison with those materials of red- and green-emission (among three general colours).[9] Since fluorine is highly electronegative and electron-withdrawing,[5] its introduction in conjugated organic molecules would generally lower the energy of both the Lowest Unoccupied Molecular Orbital (LUMO) and Highest Occupied Molecular Orbital (HOMO) energy levels.[10] Usually, the influence on the HOMO is more pronounced than the LUMO.[10b] The energy gap between HOMO and LUMO is a critical parameter in determining molecular electrical transport properties. This feature was often used to develop organic materials with higher band gaps such as blue emitters.[6a, 6c-e, 9b] The interest in fluorinated organic molecules has increased recently and understanding the chemistry of fluorinated compounds has become a major research thrust in many research groups.[11]

Noncovalent interactions attract increasing attention in modern chemical society and are considered as cornerstones in supramolecular chemistry, materials science, and even biochemistry.[12] When unsaturated organic groups are involved in noncovalent interactions, the terms "$\pi-\pi$ stacking", or more generally "$\pi-\pi$ interactions" are often used. As noted recently by Martinez and Iverson, these terms might be misleading in explaining these intermolecular forces.[13]

One of the less well understood, but important interactions in nature are aromatic interactions that involve π bonded moieties such as phenyl rings, various heterocycles, alkynes and alkenes.[14] They influence the structures of proteins,[15] DNA,[16] host-guest complexes,[17] solid materials containing

[a] School of Chemistry and Physics, University of KwaZulu-Natal, Private Bag X54001, Durban, 4000, South Africa. Email: koorbanally@ukzn.ac.za
[b] Laboratório de Planejamento e Desenvolvimento de Fármacos, Instituto de Ciências Exatas e Naturais, Universidade Federal do Pará, 66075-110, Belém, PA, Brazil.
[c] School of Chemical Engineering, University of KwaZulu-Natal, Durban 4041, South Africa.

† Supplementary Information (ESI) available: [Material and methods, computational methods, experimental procedures, reaction optimization data, ^{1}H NMR, ^{13}C NMR, ^{19}F NMR, 2D NMR, HRMS, crystallographic data and adsorption spectra of selected compounds in acetonitrile]. See DOI: 10.1039/x0xx00000x

View Article Online
DOI: 10.1039/C8CE00094H

aromatic groups,[18] and self-assembled supramolecular architectures.[18b]

The driving force for these types of self-assembly usually relies on interactions between π electron deficient and π electron rich units.[13] Both strong and weak intermolecular interactions were shown to be responsible for the 3D arrangement of molecules and hence a detailed analysis of their nature is important.[19]

Intermolecular hydrogen bonding has an important influence on the biological activity of drugs and photophysical properties of chromophores.[20] They act by an important site-specific interaction between hydrogen donor and acceptor molecules both in solid and solution phases. In recent years, the excited-state structures and dynamics of intermolecular hydrogen bonding have been widely investigated using experimental and theoretical methods.[21] In contrast, stacking of the molecules is less predictable due to the fact that variable orientations of the stacked moieties occur in order to maximise electrostatic attraction between the σ framework and π electron density of the stacked groups.[18a] Although association of several π species in solution was substantiated in some cases, there is still a need to investigate their structure in solution and relative orientation in the solid state.[22]

We herein report on the synthesis of fluorinated 4-(alkynyl)-quinolines via the Sonogashira coupling reaction. To the best of our knowledge, this is the first report of the synthesis of fluorinated 4-alkynyl-2-arylquinolines via the Sonogashira coupling reaction and there are no reports on the photophysical properties of fluorinated alkynyl quinoline heterocyclic conjugates. We also investigated the crystallographic data, quantum calculation and photo physical properties of fluorinated 4-(alkynyl)-quinolines to probe how intermolecular interactions of quinoline compounds can affect the photophysical and biological properties of the molecules.

DFT calculations were computed for ten quinoline compounds. The calculated UV absorption spectrum and other relative parameters are also discussed briefly. The frontier molecular orbitals (FMO) of quinoline compounds are presented, which are responsible for the electronic spectrum. FMO play an important role in electronic and optical properties, UV-Vis spectra and chemical reactions.

Results and discussion

In the reaction scheme, 2-substituted anilines were cyclized to 2,8-bis(substituted)quinolin-4-ol (**1**) using heat with trifluoro substituted ethyl acetoacetate in the presence of polyphosphoric acid (PPA) at 150 °C (**Scheme 1**). Quinolin-4-ol (**1**) was subsequently refluxed with fresh phosphorus oxychloride ($POCl_3$) yielding the corresponding 4-chloro-2-quinoline derivatives **2**, after which chlorine was substituted for an alkynyl group using the Sonogashira coupling reaction resulting in the formation of the target compounds **4A-S** (**Fig. 1**). The last step was carried out at 70 °C in degassed THF:water (9:1) using $Pd(OAc)_2$, xantphos as a catalyst and triethylamine (TEA) as a base.

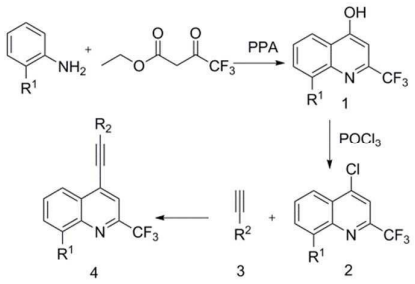

Scheme 1. Synthesis of 4-alkynyl quinolines **4**.

Optimization of reaction conditions for the final step was carried out using 4-chloroquinoline (**2**) and acetylene (**3**) as a model reaction. The effect of different Pd substrates as catalysts, solvent systems, bases and co-catalysts were examined on the Sonogashira coupling reaction. All reactions were carried out for 12 hours, as an increase in reaction time did not enhance the final yield of the product. The best reaction conditions identified occurred with $Pd(OAc)_2$ as catalyst without a co-catalyst (copper precursor), xantphos as the ligand, a 9:1 mixture of THF:water as solvent and TEA as base (**Entry 3** in **Table S1**).

Addition of co-catalysts increased yields of alkynyl dimer (**5**) reactions and decreased yields of product (**4**) (**Entries 11 and 12 in Table S1**). Acetylene precursors have to be added slowly, as fast addition leads to increased yields of the dimer (**5**). These side products are brought about by homocoupling of alkynes or Glaser type coupling, and are also known to be produced *in situ.*[29] The presence of copper as a co-catalyst was previously reported to reduce yields of Pd-catalysed Sonogashira cross-coupling reactions, which corroborates well with our findings.[24] The presence of these side products in the reaction is undesired as they create difficulties during purification of the main products.

The proposed mechanism of the copper-free reaction is shown in **scheme 2**. Phosphonates, amines and ethers (used as ligands or solvents) can reduce Pd(II) to $Pd(0)L_2$, typically via a σ-complexation-dehydropalladation-reduction elimination.[23] The catalytically active $Pd(0)L_2$ species **I** is also stabilized by the presence of ligands. The catalytic cycle begins with the oxidative addition of 4-chloroquinoline to Pd(0) resulting in the formation of Pd bound quinoline intermediate **II**, known to be the rate-determining step for the Sonogashira reaction [24]. This is followed by π co-ordination of the alkyne to Pd, resulting in an alkyne-Pd(II) complex **III**.[23b] Removal of the acetylenic proton with triethylamine results in the co-ordination of the acid carbon in acetylene to the metal **IV**. In a further step, the product **4** is released by a reductive elimination and the Pd(0)-L_2 catalyst is regenerated.

After optimizing reaction conditions on **4O**, various 4-alkynylquinolines (**Fig. 1**) were prepared via coupling of 4-chloroquinolines. In general, the yields of reactions of aliphatic alkynes (**4I, 4N, 4R** and **4S**) were lower than the aromatic alkynes (**Fig. 1**).

View Article Online
DOI: 10.1039/C8CE00094H

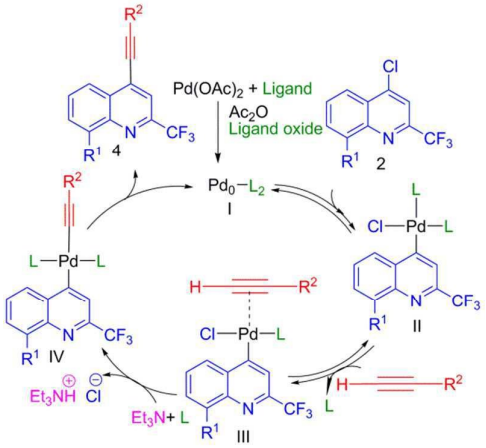

Scheme 2. Plausible mechanism for formation of 4-alkynyl-2-quinolines through a Sonogashira copper-free coupling reaction.

It was also found that the introduction of the electron withdrawing trifluoromethyl group at C-8 increased the yield (compounds **4A-4I**), while electron donating methyl groups in the same position led to a decreased yield (compounds **4J-4N**). It was observed that between the compounds **4D** and **4E** (with the trifluoromethyl groups on the introduced alkyne ring of the molecule being in the *para* and *ortho* positions respectively), the yield for the *ortho* derivative **4E** was lower.

Furthermore, the yields of the *para* and *ortho* fluoro derivatives (**4F** and **4H**) were lower than in the unsubstituted alkyne derivative (**4A**), while that of the difluoro derivative (**4G**) did not change. This could possibly be due to resonance effects of the *ortho* and *para* substituted derivatives. Electron donating *t*-butyl groups on the acetylenic aromatic ring was further shown to increase yields of those reactions (**4C**, **4L** and **4Q**).

The chemistry of phenylacetylene can only influence the last two steps of the proposed mechanism in **scheme 2**. This is when phenylacetylene is co-ordinated to the metal through π bonds. The presence of an electron donating *t*-butyl group could stabilise this co-ordinated intermediate by increasing electron density of the acetylenic bond, resulting in higher yields for the *t*-butyl derivatives.

All isolated products were characterised by NMR and mass spectrometry. The acetylenic carbon resonances are characteristic for these molecules at δ 80-100 in the ^{13}C NMR spectrum. In addition, a HMBC correlation between H-3 and the more shielded acetylenic carbon resonance as well as between the aromatic protons of the acetylenic derived moiety with the more deshielded acetylenic carbon resonance were detected, which allowed the assignment of the resonances of these two carbon atoms to be made.

X-Ray crystallography: Crystals of compounds **4A-B**, **4E**, **4I**, **4K-N**, **4P** and **4S** were grown by slow evaporation in chloroform (**Fig. 2**). The structure and conformation of the molecules was confirmed by single crystal X-ray diffraction.

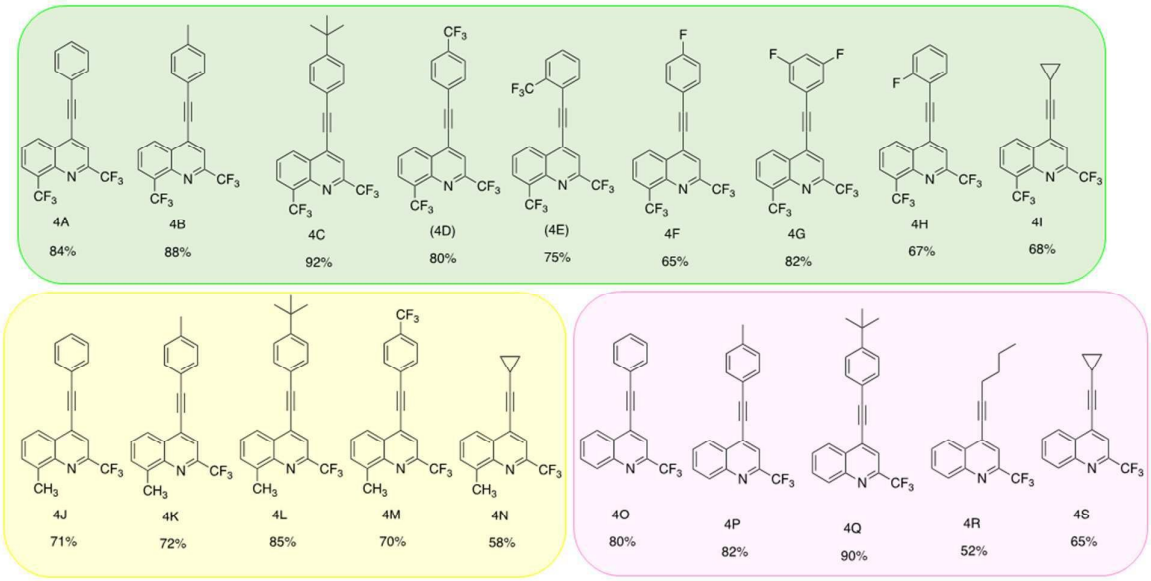

Fig. 1 Structures of Sonogoshira products formed by the substitution of chlorine with substituted alkynes: Group I: **4A-I** (2,8-disubstituted CF_3), Group II: **4J-N** (2-CF_3, 8-CH_3), Group III: **4O-S** (2-CF_3)

View Article Online
DOI: 10.1039/C8CE00094H

Journal Name

ARTICLE

The asymmetric unit of compounds **4A**, **4I, 4K** and **4P** have one molecule, compounds **2B, 4E, 4I**, **4M, 4N** and **4S** contain two molecules whilst compound **4L** has four molecules (**Figure S1**). The molecular overlay diagrams of compounds containing multiple molecules in the asymmetric unit are depicted in **Fig. S1** with their respective root mean squared deviation (RMSD). Selected bond lengths and bond angles are listed in **Table S2**. It appears that all molecules containing a phenylacetylenic group have good overlay around the quinoline scaffold and phenylacetylenic moiety with deviations arising mainly from the substituents on the phenylacetylenic group as seen in **Fig. S1**. Compound **4I** showed a minimum value for RMSD of 0.6285, indicative of bad overlaying, whilst the best overlays were seen in compounds **4N** and **4S** with RMSD of 0.1284 and 0.1289, respectively. These compounds, each contained an acetylenic moiety attached to a cyclopropyl group and it appeared that having an electron donating substituent (in **4N**) at C-8 on quinoline significantly lowered the molecular overlay's RMSD. Similarly, the presence of an electron donating substituent on the phenyl moiety in compound **4B** reduced the molecular overlay's RMSD relative to compound **4E**.

The fused quinoline rings included three main sets of planes that describe the conformations of the molecules. Three different sets of planes can be seen in all of the crystals: The first one is the fused benzene ring to the pyridine ring that formed the quinoline (P_{Bn-Q}), the second is the pyridine ring in the quinoline scaffold (P_{Py-Q}) and finally the phenyl moiety attached via a triple bond (P_{Ph}). These planes and the dihedral angles between the planes are summarised in **Table S3**. The benzene (P_{Bn-Q}) and pyridine (P_{Py-Q}) planes within the quinoline scaffold are not co-planar with dihedral angles lying between 0.4(1)°and 2.8(2)°.

The angles between the quinoline ring and phenyl planes gradually increased in the order **4A** (PhH - *para*) **> 4B** ($PhCH_3$ - *para*) **> 4E** ($PhCF_3$ - *ortho*) (**Fig. 3** and **Table S3**). By varying the electronic properties of the phenylacetylenic group, it appeared that the quinoline moiety became slightly bent, but the P_{Py-Q} - P_{Ph} and P_{Bn-Q} - P_{Ph} dihedral angles were affected to a greater extent. Surprisingly, this followed a trend observed in the molecular overlay's RMSD for compounds **4A, 4B** and **4E** as could be seen in **Fig. 3** and **Fig. 4.** On the other hand, introducing the acetylenic cyclopropyl group in **4I** resulted in less deviation from planarity in the quinoline moiety (P_{Py-Q} and P_{Bn-Q}) in comparison to the planar phenyl group such as that in **4B** and **4E**. In comparing **4B** (CF_3 at C-8), **4K** (CH_3 at C-8) and **4P** (H at C-8), in terms of deviation from planarity in the quinoline scaffold, the CF_3 group caused the most deviation followed by CH_3 and then H, which caused very little deviation from planarity (**Table S3**, **Fig. 3** and **Fig. 4**). However, the dihedral angles observed in **4K** compared to **4B** was small, whilst those in **4P** was the largest.

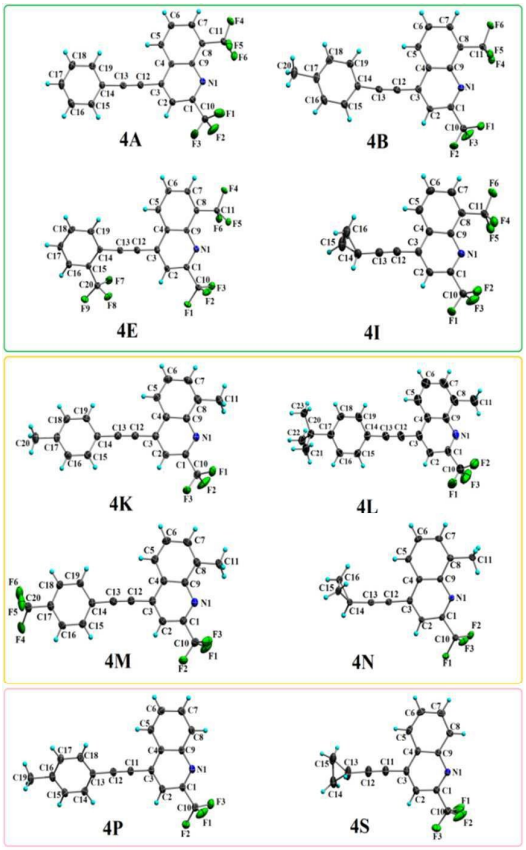

Fig. 2 ORTEP diagrams of compounds **4A-B**, **4E**, **4I**, **4K-N**, **4P** and **4S** at 50% thermal ellipsoid probability.

In the quinoline containing CF_3 and CH_3 in positions 2 and 8 of quinoline, respectively (**4K, 4L, 4M, 4N**), we observed that in contrast to our expectation, introduction of *t*-butyl and CF_3 in the *para* position of the phenyl ring (**4L, 4M**) caused less bending in the quinoline ring (P_{Py-Q} and P_{Ph-Q}). When the quinoline moiety contained CF_3 and CH_3 substituents at position 2 and 8 on the quinoline ring (in **4K, 4L** and **4M**), respectively, the strain on the quinoline unit is significantly reduced by introducing *t*-butyl (**4L**) and CF_3 (**4M**) in the *para* position (**Fig. 3** and **Fig. 4**). The strain was further reduced when the phenyl moiety was replaced with an acetylenic cyclopropyl group (**4N**). Amongst the three compounds with

View Article Online
DOI: 10.1039/C8CE00094H

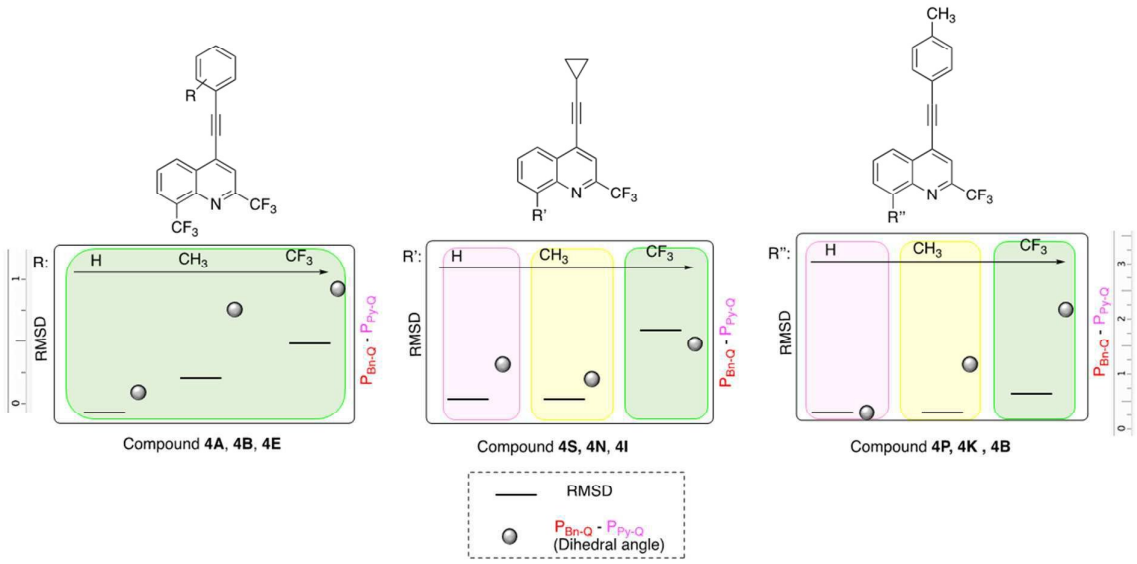

Fig. 3 A comparison of the trend of RMSD value and dihedral angles of the quinoline ring with different substituents

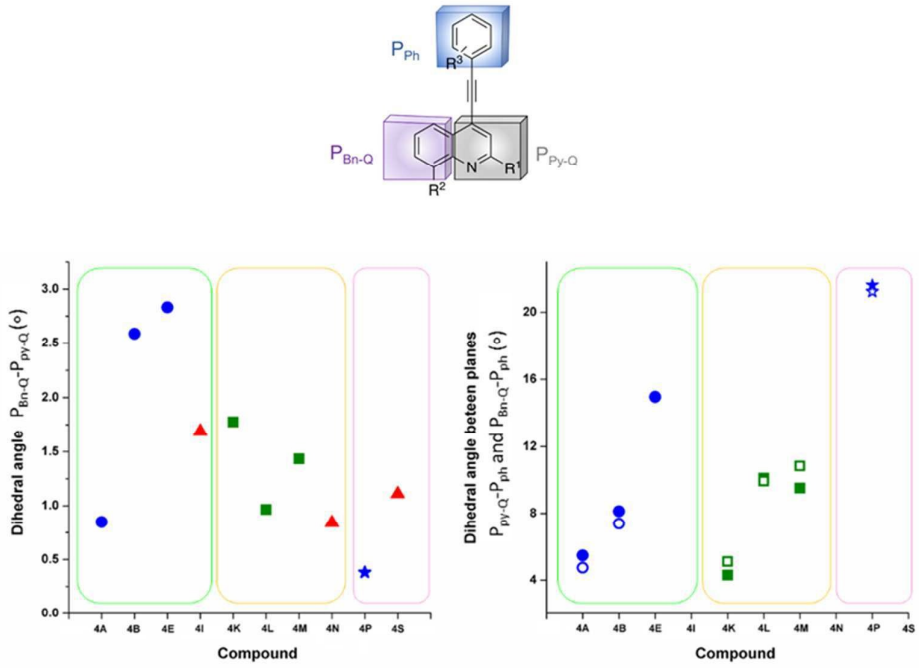

Fig. 4 Dihedral angles of **4A-B**, **4E**, **4I**, **4K-N**, **4P** and **4S:** (▲) acetylenic cyclopropyl at C-4, (solid and open ●) CF_3 at C-2 and C-8 in quinoline, (solid and open ■) CF_3 at C-2 and CH_3 at C-8 of quinoline, (solid and open ★) CF_3 at C-2 and H at C-8 of quinoline. Solid circles, squares and stars = $P_{py\text{-}Q}$-P_{ph} and open circles, squares and stars = $P_{Bn\text{-}Q}$-P_{ph}

View Article Online
DOI: 10.1039/C8CE00094H

Journal Name

ARTICLE

acetylenic cyclopropyl groups (**4I**, **4N** and **4S**), the strain in P_{Bn-Q} and P_{py-Q} was most reduced in **4N**. On the other hand, the dihedral angle between the quinoline and phenyl moieties appeared to increase with the presence of the sterically bulky *t*-butyl group (**4L**) and more electronegative CF_3 (**4M**) on the phenyl moiety.

Intermolecular interactions: The intermolecular aromatic donor-acceptor interactions and the distances between the two same molecules are depicted in **Fig. S1**. In **Fig. 5**, a comparative illustration from compound **4A** and a known similar crystal to our structures is given. As can be seen, "parallel offset" types of stacking exist for both crystal structures with similar distances between the rings.[25]

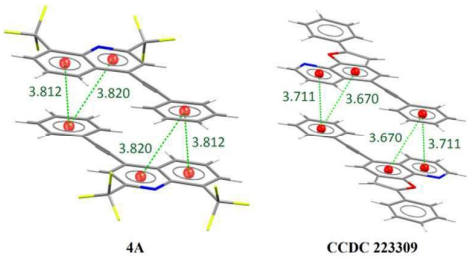

Fig. 5 Aromatic donor-acceptor interactions for compound **4A** and a similar crystal structure published previously by Hursthouse *et al.*[25]

A summary of the different types of interactions are summarised in **Tables S5** and **S6**. **Fig. S3** shows a schematic appearance of the molecules having HB. Compounds **4A-B, 4E, 4I**, **4L-N** and **4P** exhibited non-classical intermolecular C-H…F hydrogen bonding networks and no HB can be seen for compounds **4K** and **4S**. According to the summarised intermolecular interactions (**Table S6**) the maximum number of HB belonged to **4E**. The structure of this molecule deviated most from planarity (**Table S4** and **Fig. 4**) and consequently possessed the most number of fluorine atoms (P_{Bn-Q} -P_{Py-Q} (2.831) P_{Py-Q}-P_{Ph} (14.958) P_{Bn-Q}-P_{Ph} (14.788)). Thus, it can be suggested that an increase in fluorine atoms in an organic backbone increases the presence of non-conventional inter and intra-molecular hydrogen bonding, consistent with our previous results.[11] In spite of the rigid structure of organic compounds like quinoline, fluorine can alter their 3D structure through these intermolecular interactions.

Photophysical properties: In order to investigate the photophysical properties of the quinoline-based alkyne substituted derivatives, the UV and fluorescence spectra (**Table 1**) in acetonitrile were recorded. Most compounds displayed two absorption peaks in the UV spectra at 230–244 and 315–340 nm, which were ascribed to π–π* and n-π* transitions respectively.[26]

Spectral characteristics such as absorption (λ_{abs}), emission (λ_{em}) and extinction coefficient (ε) of all compounds (**4A-B**, **4E**, **4I**, **4K-N**, **4P** and **4S**) were measured in acetonitrile and the results presented in **Table 1** and **Figs S4** and **S5**. Changes in the substituents at C-8 and in the acetylenic group are seen to cause notable changes in the absorption and emission spectra (**Fig. S4** and **Fig. S5**). This is possibly due to their different electron withdrawing and donating abilities.[26]

Amongst the group I molecules possessing CF_3 at C-2 and C-8 in quinoline, a bathochromic shift occurred when a more electron donating methyl group (**4B**) was substituted on the aromatic acetylenic moiety. The electron withdrawing CF_3 group (**4E**) had almost no effect in comparison to **4A**. Replacing the conjugated acetylenic phenyl group with an acetylenic cyclopropyl group, caused a hypsochromic shift to 313 (nm). The same trend can be seen in group II (CF_3 at C-2 and CH_3 at C-8 of quinoline). In this case, the more bulky *t*-butyl group (**4L**) did not have any effect in comparison to **4K,** however the electron withdrawing CF_3 group (**4M**) resulted in a hypsochromic shift, almost similar to when an acetylenic cyclopropane group (**4N**) occurred at the same position. A similar trend was observed in group III (CF_3 at C-2, H at C-8 of quinoline) from **4P** to **4S**, a hypsochromic shift occurring when the toluene moiety was replaced by a cyclopropane moiety. For differing substituents at C-8, in comparison to **4P** (H at C-8) bathochromic shifts were seen for both electron withdrawing **4B** (CF_3 at C-8) and electron donating substituents **4K** (CH_3 at C8).

In general, decreasing the conjugation and introducing electron withdrawing substituents on the acetylenic moiety resulted in a hypsochromic shift. Most compounds produced emission spectra in the range for blue emitters (405–442 nm)[27] in acetonitrile and solid phases at room temperature.

Computational analysis: To gain more insight into the nature of the electronic transition, the energy level diagrams of a series of dominating frontier molecular orbitals (FMOs) and contour plots of the HOMO/LUMO are presented for **4A-B, 4E, 4I, 4K-N, 4P** and **4S** in the ground state, along with the energy gaps (ΔE_{H-L}) between HOMOs and LUMOs (**Fig. 6**). The energy gap was considered as a reactivity indicator. A reactive molecule is characterized by a small energy gap. The energies

View Article Online
DOI: 10.1039/C8CE00094H

Journal Name

ARTICLE

Table 1. : Summarized details from UV and florescence spectra of compounds **4A, 4B, 4E, 4I, 4K, 4L, 4M, 4N, 4P** and **4S**

Compound	λ_{max1}/nm	λ_{max2}/nm*	ε/ x 10^4 L mol^{-1} cm^{-1}		$\lambda_{Emission}$/nm *		Stoke's shift/nm		E_{excit}/eV*
			λ_{max1}	λ_{max2}	$\lambda_{solution}$	$\lambda_{solid-state}$	$\lambda_{solution}$	$\lambda_{solid-state}$	
4A	233	327	2.70	1.76	404.5	427.5	77.5	100.5	3.810
4B	234	347	6.56	4.35	434.5	352.5	87.5	5.5	3.580
4E	233	326	3.84	2.65	385.0	385.0	59.0	59.0	3.810
4I	230	313	3.80	1.45	441.0	417.0	128.0	104.0	3.968
4K	244	340	4.51	2.14	404.5	-	64.5	-	3.610
4L	244	340	4.06	1.91	402.5	425.5	62.5	85.5	3.642
4M	233	325	4.36	2.94	328.0	429.5	3.0	104.5	3.821
4N	241	323	4.34	0.969	324.0	402.5	1.0	79.5	3.845
4P	239	331	5.59	3.11	406.0	399.5	75.0	68.5	3.752
4S	237	315	5.98	2.33	431.0	386.5	116.0	71.5	3.955

* E_{excit} is calculated using λ_{max2}/nm

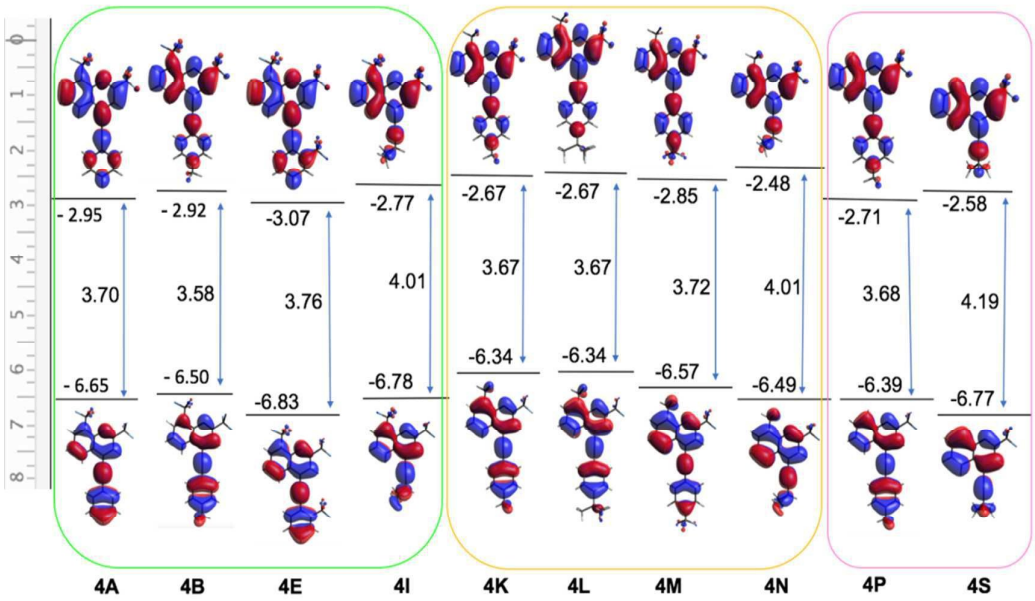

Fig. 6 HOMO and LUMO energy levels of compounds **4A-B**, **4E**, **4I**, **4K-N**, **4P** and **4S**

View Article Online
DOI: 10.1039/C8CE00094H

Journal Name

ARTICLE

and distributions of the FMOs help in demonstrating the chemical reactivity, active site/s, and kinetic stability of the molecules. In order to evaluate the energetic behaviour of the quinoline compounds under investigation, the FMO calculations were carried out at B3LYP/6-311++G** in gas phase, and in acetonitrile, as solvent. The results were summarized in **Table S7**.

The energy gap (E.G.) between the HOMO and LUMO orbitals is a critical parameter in determining molecular transport properties. It is a measure of electron conductivity. In fact, a large HOMO-LUMO gap means high molecular stability and molecular charge transfer from electron-donor centre to electron-acceptor centre through a π-conjugated path. In our set of compounds, the HOMO-LUMO gap is quite small (and hence reactive) and the experimental values compared quite well with theoretical values, except for **4N** and **4S (Fig. 7)**.

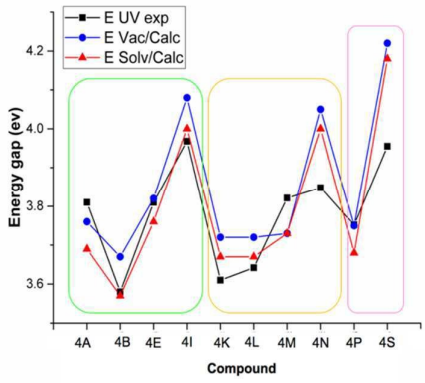

Fig. 7 Comparison of energy level gap (ev) of experimental and computation in vacuum and solvent

Conclusions

The synthesis of 19 novel derivatives of fluoroquinoline compounds was achieved using the Sonogashira coupling reaction. SC-XRD crystals of 10 of the synthesised compounds were successfully carried out. Variation of substituents at C-4 (substituted aromatic or cylcopropane acetylenic groups) and C-8 (CF_3, CH_3 or H) enabled us to study the influence of these modifications on their structures. SC-XRD, UV-Vis, and computational data indicated that fluorine atoms inserted at selected positions on the structure could alter their planarity, π…π stacking and number of existing non-conventional hydrogen bonding interactions. Compound **4E** was found to be highly non-planar and had few aromatic donor-acceptor interactions, probably due to a high number of non-conventional hydrogen bonds detected in its structure. Thus, fluorine has good potential to modify the 3D structures of organic compounds, even highly inflexible ones such as quinoline. The study of FMO using computational techniques was in good agreement with experimental data and showed a small energy gap between HOMO and LUMO.

Conflicts of interest

We do not have any conflicts of interest.

Acknowledgements

This research was supported by grants from the National Research Foundation (NRF), South Africa and was supported by the South African Research Chairs Initiative of the Department of Science and Technology.

References

1. (a) S. Calus, E. Gondek, A. Danel, B. Jarosz and A. V. Kityk, *Opt. Commun.*, 2007, **271**, 16-23; (b) E. Gondek, A. Danel and I. V. Kityk, *Philos. Mag.*, 2010, **90**, 2677-2685; (c) S. Calus, E. Gondek, A. Danel, B. Jarosz, A. Pokladko and A. V. Kityk, *Mater. Lett.*, 2007, **61**, 3292-3295; (d) E. Gondek, A. Danel, J. Niziol, P. Armatys, I. V. Kityk, P. Szlachcic, M. Karelus, T. Uchacz, J. Chwast and G. Lakshminarayana, *J. Lumin.*, 2010, **130**, 2093-2099.
2. (a) S. Kappaun, C. Slugovc and E. J. W. List, *Int. J. Mol. Sci.*, 2008, **9**, 1527-1547; (b) J. Park, J. S. Park, Y. G. Park, J. Y. Lee, J. W. Kang, J. Liu, L. M. Dai and S. H. Jin, *Org. Electron.*, 2013, **14**, 2114-2123; (c) J. Y. Li, R. J. Wang, R. X. Yang, W. Zhou and X. Wang, *J. Mater. Chem. C*, 2013, **1**, 4171-4179; (d) C. J. Tonzola, M. M. Alam, W. Kaminsky and S. A. Jenekhe, *J. Am. Chem. Soc.*, 2003, **125**, 13548-13558.
3. S. Wong, H. Ma, A. K. Y. Jen, R. Barto and C. W. Frank, *Macromolecules*, 2003, **36**, 8001-8007.
4. (a) Y. Mizuno, I. Takasu, S. Uchikoga, S. Enomoto, T. Sawabe, A. Amano, A. Wada, T. Sugizaki, J. Yoshida, T. Ono and C. Adachi, *J. Phys. Chem. C*, 2012, **116**, 20681-20687; (b) F. Babudri, G. M. Farinola, F. Naso and R. Ragni, *Chem. Commun.*, 2007, DOI: 10.1039/b611336b, 1003-1022; (c) Z. F. Li, Z. X. Wu, W. Fu, P. Liu, B. Jiao, D. D. Wang, G. J. Zhou and X. Hou, *J. Phys. Chem. C*, 2012, **116**, 20504-20512.
5. D. O'Hagan, *Chem. Soc. Rev.*, 2008, **37**, 308-319.
6. (a) X. H. Yang, Z. X. Wang, S. Madakuni, J. Li and G. E. Jabbour, *Adv. Mater.*, 2008, **20**, 2405-2409; (b) Z. X.

View Article Online
DOI: 10.1039/C8CE00094H

Wang, E. Turner, V. Mahoney, S. Madakuni, T. Groy and J. A. Li, *Inorg. Chem.*, 2010, **49**, 11276-11286; (c) Z. Wang, E. Turner, V. Mahoney, S. Madakuni, T. Groy and J. Li, *Inorg. Chem.*, 2010, **49**, 11276-11286; (d) C.-H. Yang, M. Mauro, F. Polo, S. Watanabe, I. Muenster, R. Froehlich and L. De Cola, *Chem. Mater.*, 2012, **24**, 3684-3695; (e) S. Lee, S.-O. Kim, H. Shin, H.-J. Yun, K. Yang, S.-K. Kwon, J.-J. Kim and Y.-H. Kim, *J. Am. Chem. Soc.*, 2013, **135**, 14321-14328; (f) S. Shao, J. Ding, L. Wang, X. Jing and F. Wang, *J. Am. Chem. Soc.*, 2012, **134**, 20290-20293.

7. (a) W. T. Li, S. Abrecht, L. Q. Yang, S. Roland, J. R. Tumbleston, T. McAfee, L. Yan, M. A. Kelly, H. Ade, D. Neher and W. You, *J. Am. Chem. Soc.*, 2014, **136**, 15566-15576; (b) N. Wang, Z. Chen, W. Wei and Z. H. Jiang, *J. Am. Chem. Soc.*, 2013, **135**, 17060-17068; (c) J. S. Kim, Y. Lee, J. H. Lee, J. H. Park, J. K. Kim and K. Cho, *Adv. Mater.*, 2010, **22**, 1355-1360.
8. (a) T. Lei, J. H. Dou, Z. J. Ma, C. H. Yao, C. J. Liu, J. Y. Wang and J. Pei, *J. Am. Chem. Soc.*, 2012, **134**, 20025-20028; (b) J. H. Oh, S. L. Suraru, W. Y. Lee, M. Konemann, H. W. Hoffken, C. Roger, R. Schmidt, Y. Chung, W. C. Chen, F. Wurthner and Z. N. Bao, *Adv. Funct. Mater.*, 2010, **20**, 2148-2156.
9. (a) T. Fleetham, Z. X. Wang and J. Li, *Org. Electron.*, 2012, **13**, 1430-1435; (b) S. Y. Shao, J. Q. Ding, L. X. Wang, X. B. Jing and F. S. Wang, *J. Am. Chem. Soc.*, 2012, **134**, 15189-15192; (c) T. Fleetham, J. Ecton, Z. X. Wang, N. Bakken and J. Li, *Adv. Mater.*, 2013, **25**, 2573-2576.
10. (a) J. L. Bredas and A. J. Heeger, *Chem. Phys. Lett.*, 1994, **217**, 507-512; (b) W. Wan, H. Wang, H. Lin, J. Wang, Y. Jiang, H. Jiang, S. Zhu, Z. Wang and J. Hao, *Dyes Pigm.*, 2015, **121**, 138-146.
11. (a) D. O'Hagan, *J. Fluorine Chem.*, 2010, **131**, 1071-1081; (b) S. Alapour, D. Ramjugernath and N. A. Koorbanally, *RSC Adv.*, 2015, **5**, 83576-83580; (c) S. H. Li, P. Wu, J. E. Moses and K. B. Sharpless, *Angew. Chem. Int. Ed.*, 2017, **56**, 2903-2908; (d) K. G. Andrews, R. Faizova and R. M. Denton, *Nat. Commun.*, 2017, **8**, 15913; (e) S. M. Banik, K. M. Mennie and E. N. Jacobsen, *J. Am. Chem. Soc.*, 2017, **139**, 9152-9155; (f) W. Chen, N. Guo, M. Qi, H. Dai, M. Hong, L. Guan, X. Huan, S. Song, J. He, Y. Wang, Y. Xi, X. Yang, Y. Shen, Y. Su, Y. Sun, Y. Gao, Y. Chen, J. Ding, Y. Tang, G. Ren, Z. Miao and J. Li, *Eur. J. Med. Chem.*, 2017, **138**, 514-531; (g) S.-Q. Peng, X.-W. Zhang, L. Zhang and X.-G. Hu, *Org. Lett.*, 2017, DOI: 10.1021/acs.orglett.7b02866, Ahead of Print; (h) A. Quintard and J. Rodriguez, *ACS Catal.*, 2017, **7**, 5513-5517; (i) C. D. Sessler, M. Rahm, S. Becker, J. M. Goldberg, F. Wang and S. J. Lippard, *J. Am. Chem. Soc.*, 2017, **139**, 9325-9332; (j) J. Wang, S. Jia, K. Okuyama, Z. Huang, E. Tokunaga, Y. Sumii and N. Shibata, *J. Org. Chem.*, 2017, DOI: 10.1021/acs.joc.7b01908; (k) J.-b. Wang, A. Ilie, S. Yuan and M. T. Reetz, *J. Am. Chem. Soc.*, 2017, **139**, 11241-11247; (l) S. Alapour, M. D. Farahani, J. R. A. Silva, C. N. Alves, H. B. Friedrich, D. Ramjugernath and N. A. Koorbanally, *Monatsh. Chem.*, 2017, **148**, 2061-2068.
12. (a) S. Grimme, *Angew. Chem., Int. Ed.*, 2008, **47**, 3430-3434; (b) J. Cerny and P. Hobza, *Phys. Chem. Chem. Phys.*, 2007, **9**, 5291-5303; (c) N. Kannan and S. Vishveshwara, *Protein Eng.*, 2000, **13**, 753-761.
13. C. R. Martinez and B. L. Iverson, *Chem. Sci.*, 2012, **3**, 2191-2201.
14. (a) S. M. M. Sony and M. N. Ponnuswamy, *Cryst. Growth Des.*, 2006, **6**, 736-742; (b) M. L. Waters, *Curr. Opin. Chem. Biol.*, 2002, **6**, 736-741.
15. (a) S. K. Burley and G. A. Petsko, *Science*, 1985, **229**, 23-28; (b) C. A. Hunter, J. Singh and J. M. Thornton, *J. Mol. Biol.*, 1991, **218**, 837-846.
16. S. Neidle, *Principles of Nucleic Acid Structure*, Elsevier Science, 2010.
17. (a) B. Askew, P. Ballester, C. Buhr, K. S. Jeong, S. Jones, K. Parris, K. Williams and J. Rebek, Jr., *J. Am. Chem. Soc.*, 1989, **111**, 1082-1090; (b) D. B. Smithrud and F. Diederich, *J. Am. Chem. Soc.*, 1990, **112**, 339-343; (c) C. A. Hunter, *Chem. Soc. Rev.*, 1994, **23**, 101-109.
18. (a) C. A. Hunter and J. K. M. Sanders, *J. Am. Chem. Soc.*, 1990, **112**, 5525-5534; (b) C. G. Claessens and J. F. Stoddart, *J. Phys. Org. Chem.*, 1997, **10**, 254-272.
19. D. Dey and D. Chopra, *CrystEngComm*, 2015, **17**, 5288-5298.
20. (a) S. Dajnowicz, J. M. Parks, X. Hu, K. Gesler, A. Y. Kovalevsky and T. C. Mueser, *J. Biol. Chem.*, 2017, **292**, 5970-5980; (b) D. Sahoo, M. G. Quesne, S. P. de Visser and S. P. Rath, *Angew. Chem., Int. Ed.*, 2015, **54**, 4796-4800; (c) M. Yoosefian, H. Karimi-Maleh and A. L. Sanati, *J. Chem. Sci. (Berlin, Ger.)*, 2015, **127**, 1007-1013; (d) M. Yoosefian, H. Karimi-Maleh and A. L. Sanati, *J. Chem. Sci.*, 2015, **127**, 1007-1013; (e) P. Trojanowski, J. Plotner, C. Grunewald, F. F. Graupner, C. Slavov, A. J. Reuss, M. Braun, J. W. Engels and J. Wachtveitl, *Phys. Chem. Chem. Phys.*, 2014, **16**, 13875-13888; (f) P. Trojanowski, J. Ploetner, C. Gruenewald, F. F. Graupner, C. Slavov, A. J. Reuss, M. Braun, J. W. Engels and J. Wachtveitl, *Phys. Chem. Chem. Phys.*, 2014, **16**, 13875-13888.
21. P. Song and F.-C. Ma, *Int. Rev. Phys. Chem.*, 2013, **32**, 589-609.
22. (a) B. Olenik, R. Boese and R. Sustmann, *Cryst. Growth Des.*, 2003, **3**, 175-181; (b) D. L. Reger, R. F. Semeniuc, C. Pettinari, F. Luna-Giles and M. D. Smith, *Cryst. Growth Des.*, 2006, **6**, 1068-1070; (c) J. A. Marsden, J. J. Miller, L. D. Shirtcliff and M. M. Haley, *J. Am. Chem. Soc.*, 2005, **127**, 2464-2476.
23. (a) E.-I. Negishi and L. Anastasia, *Chem. Rev.*, 2003, **103**, 1979-2017; (b) R. Chinchilla and C. Najera, *Chem. Rev.*, 2007, **107**, 874-922.
24. V. Polshettiwar, T. Asefa and G. Hutchings, *Nanocatalysis: Synthesis and Applications*, Wiley, New Jersey, First edn., 2013.
25. M. B. Hursrhouse, T. Gelbrich and I. R. Butler, CCDC 223309: CSD Communication, 2003, DOI: 10.5517/cc7hcjl.
26. Q. Li, B. Li, B. Liu and M. Yu, *J. Chem. Res.*, 2010, **34**, 379-381.
27. M. R. Zhu and C. L. Yang, *Chem. Soc. Rev.*, 2013, **42**, 4963-4976.

View Article Online
DOI: 10.1039/C8CE00094H

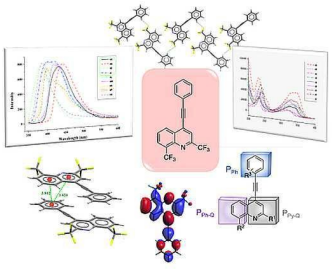

Addition of fluorine to the quinoline structure was found to decrease its intermolecular interactions and influence its 3D structure.